

**Why Some Metal Ions Spontaneously Form Nanoparticles in Water
Microdroplets? Disentangling the Contributions of Air–Water Interface
and Bulk Redox Chemistry**

Muzzamil Ahmad Eatoo^{a,b,c,d}, Nimer Wehbe^e, Najeh Kharbatia^b, Xianrong Guo^e, Himanshu
Mishra^{a,b,c,d*}

^aEnvironmental Science and Engineering (EnSE) Program, Biological and Environmental
Science and Engineering (BESE) Division, Water Desalination and Reuse Center (WDRC)

^bWater Desalination and Reuse Center (WDRC),

King Abdullah University of Science and Technology (KAUST), Thuwal, 23955-6900,
Kingdom of Saudi Arabia

^cCenter for Desert Agriculture (CDA), King Abdullah University of Science and Technology
(KAUST), Thuwal 23955-6900, Saudi Arabia

^dInterfacial Lab (iLab), King Abdullah University of Science and Technology (KAUST),
Thuwal 23955-6900, Saudi Arabia

^eCore Labs, King Abdullah University of Science and Technology (KAUST), Thuwal 23955-
6900, Saudi Arabia

*Correspondence: himanshu.mishra@kaust.edu.sa

Abstract

Water microdroplets containing 100 μM HAuCl_4 have been shown to reduce gold ions into gold nanoparticles spontaneously. It has been suggested that this chemical transformation is driven by ultrahigh electric fields at the air–water interface, albeit without mechanistic insight. We investigated the fate of several metallic salts in water, methanol, ethanol, and acetonitrile in bulk and microdroplets. This revealed that when HAuCl_4 (or PtCl_4) is added to bulk water (or methanol or ethanol), metal NPs appear spontaneously. Over time, the nanoparticles grow in bulk, as evidenced by the solutions' changing colors. If the same bulk solution is sprayed pneumatically and collected, the NP size has no significant enhancement. Interestingly, the reduction of metal ions is accompanied by the oxidation of water (or alcohols); however, these redox reactions are minimal in acetonitrile. We establish that the spontaneous reduction of metal ions is (i) not limited to water or gold ions, (ii) not driven by the air-water interface of microdroplets, and (iii) appears to be a general phenomenon for solvents containing hydroxyl groups. These results advance our understanding of liquids in general and should be relevant in soil chemistry, biogeochemistry, electrochemistry, and green chemistry.

Introduction

Biochemistry, chemistry, and chemical engineering textbooks often limit the role of water in chemical reactions to dissolving/hydrating molecules and ions¹⁻³; however, this view is rapidly evolving⁴⁻⁹. In the last two decades, experimental and computational studies have revealed that the skin of water – the air-water interface – and water–hydrophobe interfaces, in general, have anomalous features such as enhanced speciation of ions^{10, 11} and electrified interfaces¹²⁻¹⁵. Several studies have reported on orders of magnitude faster (e.g., 10^2 – $10^6\times$) reaction rates in water microdroplets compared with the bulk phase, thereby expanding the function of aqueous interfaces in chemical transformations beyond heat and mass transfer^{5, 16-24}. This exciting field – Microdroplet Chemistry – has emerged as a frontier in chemical science with potential implications for atmospheric aerosol²⁵; sea sprays²⁶; disease transmission^{27, 28}; life's origins^{16, 19, 29}; chemistries in clouds, fog, smog, and dew³⁰⁻³²; soil processes³³; green chemistry¹⁸; hospital disinfection³⁴; food industry³⁵; and fizzy beverages³⁶; also, one may expect similar trends in microbubbles/foam in fermenter broths³⁷, wastewater treatment^{38, 39}, and electrochemistry^{40, 41}.

While much excitement exists, several claims for purely interfacial chemistry being responsible for the rate enhancement have been challenged. This is because a vast majority of

reports exploit electrospray ionization mass spectrometry (ESIMS), which entails rapid solvent evaporation, solute concentration, temperature, and electric field gradients, etc., conditions that are far from thermodynamic equilibrium and, therefore, not representative of common systems^{20, 23, 42, 43}. For instance, the emergence of superacid chemistry in the microdroplets of mildly acidic water ($\text{pH} < 4$)^{44, 45} and the formation of abiotic sugar phosphates in water microdroplets¹⁶, which have been challenged by Mishra & co-workers⁴⁶⁻⁴⁸ and Wilson & co-workers⁴⁹, respectively (for recent reviews on this subject, see Ref.^{15, 24, 50, 51}). Controversial reports on microdroplet chemistry are not limited to ESIMS alone. For instance, recently, Zare & co-workers claimed that the air–water interface of microdroplets spontaneously generates H_2O_2 ⁵²⁻⁵⁵, and the reported amounts varied from ~ 1 ppm or $30\ \mu\text{M}$ (in 2019 for pneumatically sprayed droplets)⁵² to $114\ \mu\text{M}$ (in 2020 for condensed droplets)⁵⁴ to $180\ \mu\text{M}$ (in 2021 for microdroplets condensed at 50% relative humidity)⁵³ to $0.3\text{--}1.5\ \mu\text{M}$ (in 2022 for sprayed droplets in the zone-free gas environment, which increased four folds if $\text{O}_2(\text{g})$ was used to spray water pneumatically)⁵⁵. As for mechanistic insights, the computer simulations by Head-Gordon & co-workers^{56, 57} suggested the emergence of instantaneous ultrahigh electric fields at the air–water interface that may drive H_2O_2 formation, while the simulations of Ruiz-Lopez and co-workers⁵⁰ suggested that the local electric field was smaller at the air–water interface compared to the bulk and emphasized the role of significant fluctuations of the electrostatic potential. Cooks and co-workers have speculated (basing it on Amotz’s commentary⁵⁸ on a paper by Roke & co-workers on water–oil electrification¹²) that the air–water interface of microdroplets promotes the formation of water radical cations H_2O^{+*} and anions H_2O^{-*} , which upon separation during spraying drive redox reactions²⁴. Colussi also proposed a similar mechanism whereby spraying yielded a small fraction of oppositely charged droplets, i.e., comprising excess H_3O^+ and OH^- . These droplets collided to form OH^* and H^* radicals⁵⁹.

Our experimental investigation uncovered that the first two reports from Zare & co-workers, claiming $30\text{--}114\ \mu\text{M}$ H_2O_2 formation, were, in fact, reporting artifacts resulting from ambient ozone gas^{60, 61}. In their latest paper, Zare & co-workers have acknowledged their mistake^{55, 62, 63}. When they repeated their experiments in an ozone-free environment^{55, 62, 63} and found $\sim 0.3\text{--}1.5\ \mu\text{M}$ $\text{H}_2\text{O}_2(\text{aq})$ in sprayed microdroplets and, therefore, doubled down on their original claim; also, they noted that the $\text{H}_2\text{O}_2(\text{aq})$ concentration in water microdroplets increases around four times if the nebulizing gas was changed from $\text{N}_2(\text{g})$ to $\text{O}_2(\text{g})$. Our latest report demonstrated that this trace $\text{H}_2\text{O}_2(\text{aq})$ formation (i.e., $0.3\text{--}1.5\ \mu\text{M}$) takes place at the water–solid interface and not the air–water interface⁶⁴. This happens as the dissolved oxygen

($\text{O}_2(\text{aq})$) gets reduced and the surface gets oxidized, i.e., if $\text{O}_2(\text{aq})$ is eliminated from the water, $\text{H}_2\text{O}_2(\text{aq})$ is not observed within a detection limit of 50 nM. Notably, the amount of $\text{H}_2\text{O}_2(\text{aq})$ formed at various water–solid interfaces (e.g., stainless steel, Mg, Ti, Si, and SiO_2) varies in accordance with the Galvanic series. Our findings thus disprove the mechanisms for the spontaneous $\text{H}_2\text{O}_2(\text{aq})$ formation proposed by Zare and co-workers^{27, 52-55, 65, 66}, Head-Gordon and co-workers^{56, 57}, Cooks and co-workers²⁴, and Colussi⁵⁹. Recently, Nguyen & co-workers⁶⁷ and Koppenol & co-workers⁶⁸ have also refuted the $\text{H}_2\text{O}_2(\text{aq})$ generation claims in condensed droplets. Given the inconsistent experimental results and multiplicity of explanations for the microdroplet phenomena, a careful and case-by-case assessment of chemistries at the air–water interface and their implications in natural and applied sciences is warranted.

Based on these findings, we investigate another claim from Zare & co-workers on the spontaneous reduction of $\text{Au}^{3+}(\text{aq})$ to Au nanoparticles (Au NPs) in water microdroplets containing chloroauric acid (HAuCl_4 , 100 μM concentration)⁶⁹. This phenomenon is also speculated to exclusively occur at the air–water interface of microdroplets due to ultrahigh interfacial electric fields, i.e., without a reducing agent or an electrical voltage required for the bulk water phase. However, it is not entirely clear what the special role of the water interface or the gold ions is in this process or if $\text{H}_2\text{O}_2(\text{aq})$ formation is implicated in this phenomenon also⁷⁰. It has been noted that gold nanoparticles can be formed in bulk water by applying microwaves⁷¹; others have shown that light can impact the reduction of Fe^{3+} to Fe^{2+} in water⁷². Herein, we present the results of our investigation along the following lines of inquiry:

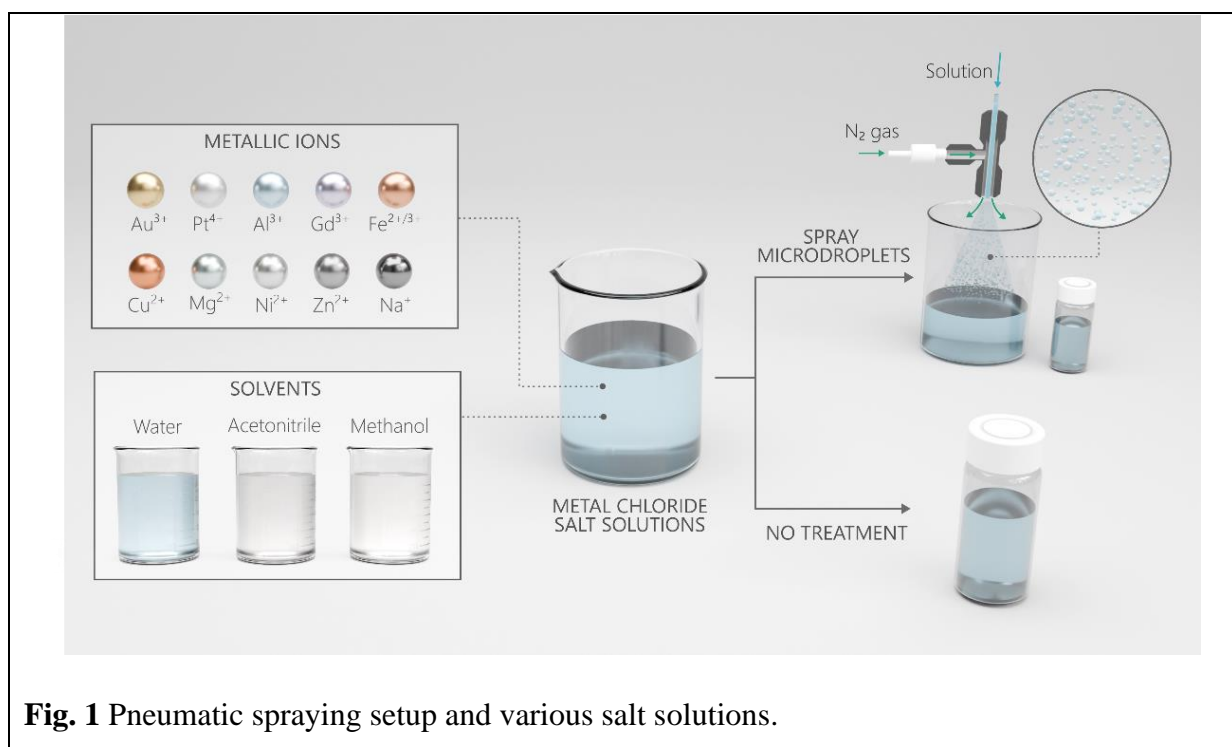
1. Is the spontaneous reduction of gold in water limited only to water microdroplets, or does it also occur in bulk water? Note: the microdroplets are produced pneumatically.
2. If gold ions get spontaneously reduced inside water, does water get oxidized?
3. What are the effects of gold ion concentration and water pH on the NP formation?
4. Do other metallic ions, e.g., Pt^{4+} and Fe^{3+} , also exhibit this behavior?
5. Does water have unique properties, or can other common liquids such as alcohols also drive the spontaneous reduction of metallic ions? If so, what are the reaction byproducts?
6. What are the fundamental molecular mechanisms underlying these chemical transformations?

We observed that when Au^{3+} (or Pt^{4+} or Fe^{3+}) was added to water, methanol, or ethanol, they were spontaneously reduced in the bulk phase as well as in water microdroplets. In fact, in this study, whenever NPs formed for a specific salt–solvent system, they formed both in the bulk

and microdroplets. In other words, we found no scenario wherein the spontaneous reduction occurred exclusively inside microdroplets but not in bulk.

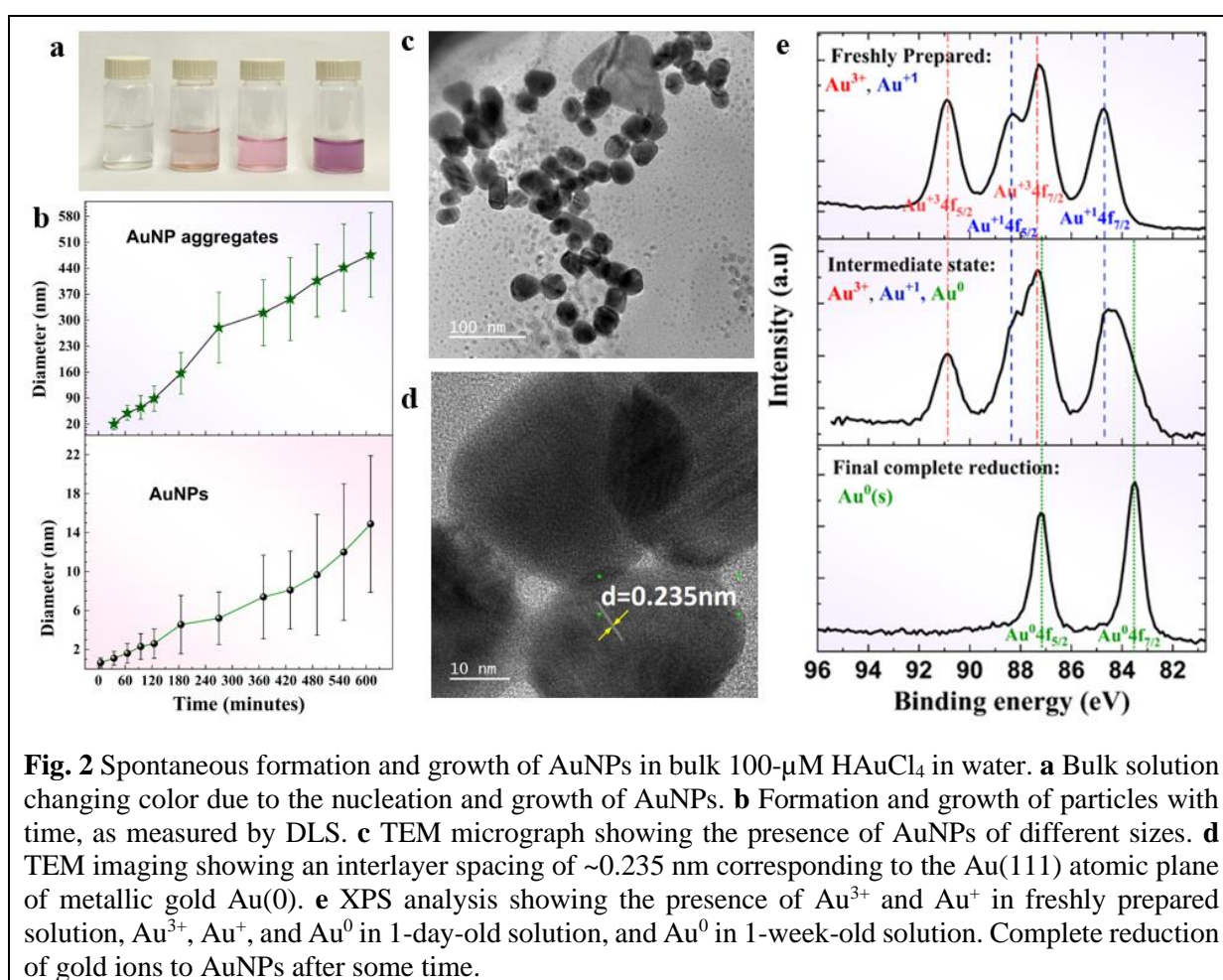
Results

In this work, we used MilliQ Advantage 10 (18 M Ω -cm, 3 ppb) deionized water, albeit the results were identical with HPLC grade water. Microdroplets were obtained via pneumatic nebulization following the experimental setup of Zare et al.⁶⁹. The spray device comprised two concentric capillaries, and the solution was injected through a 0.1-mm-wide inner stainless-steel capillary at a rate of 25 μ l/min. The solution was sheared via high-pressure dry N₂ gas flowing through the outer concentric capillary at 100 psi, forming a microdroplet stream (Supplementary Fig. S1).



The effects of the air–water interface on NP formation were analyzed by spraying 100- μ M aqueous HAuCl₄ solution via pneumatic nebulization, which yielded microdroplets of an average size of \sim 20 μ m (Supplementary Fig. S1). The microdroplets were collected in clean glass vials and transferred into transmission electron microscopy (TEM) grids for TEM imaging and SiO₂/Si wafers for scanning electron microscopy (SEM) analysis, which revealed NP formation (Supplementary Fig. S2). Moreover, the transparent mother solution (100- μ M aqueous HAuCl₄ stored at 22°C inside a laboratory) changed its color to red in a few (2-3) days and blue in a few (2-3) weeks (Fig. 2(a)). The TEM analysis of samples drawn from the mother

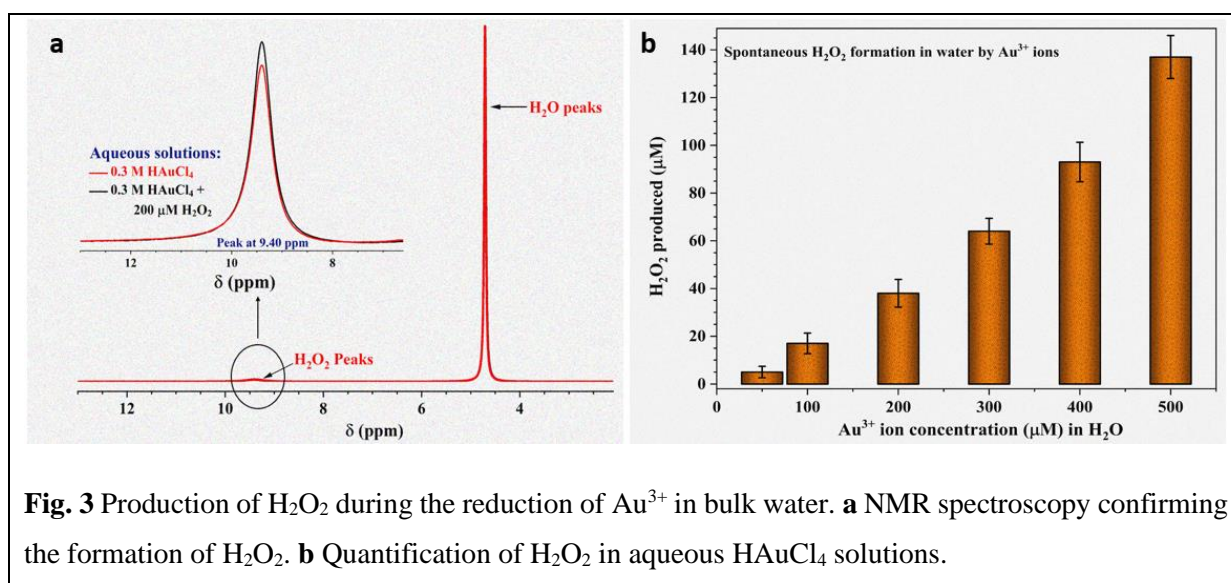
solutions revealed the presence of gold NPs (Figs. 2c,d, and S3). Dynamic light scattering (DLS) showed the appearance of a bimodal nanoparticle size distribution in the freshly prepared solutions (Fig. 2(b)). X-ray photoelectron spectroscopy compared the oxidation states of gold in the newly prepared and one-week-old solutions (Fig. 2(e), Methods). The oxidation state of gold in the freshly prepared solutions was +3 and +1, whereas that in the 1-week-old samples was 0. Irrespective of the duration of XPS measurements, an oxidation state of +3 was not recorded; this indicated that the reduction was spontaneous. These results demonstrate that the reduction of gold ions can occur spontaneously in bulk water and is not exclusive to the microdroplet environment.



However, whether the microdroplet environment, i.e., the air–water interface, considerably accelerated the rate of reduction and nanoparticle formation compared with the bulk phase was further investigated. To this end, bulk solutions of the same concentration (100- μ M HAuCl₄) but different ages, i.e., varying from seconds to minutes to hours, were pneumatically sheared into water microdroplets. The flying microdroplets were then intercepted and collected (in the liquid state, i.e., before complete evaporation) and analyzed

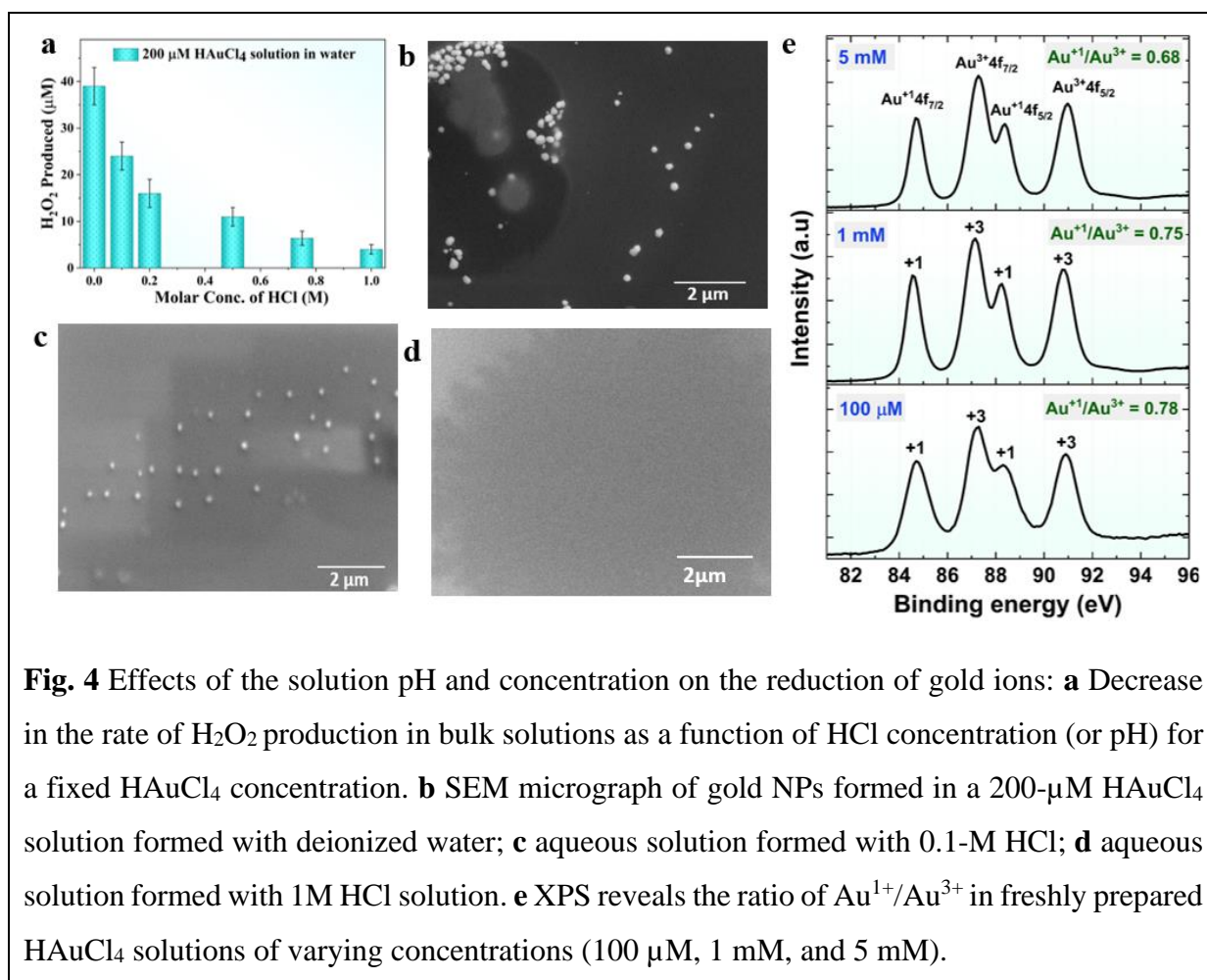
via DLS. The observed particle size distributions were compared against those of the mother solution (Fig. S4). Results revealed that the microdroplets afforded no significant enhancement in the particle sizes over the bulk phase, demonstrating that microdroplets do not have any significant effect on the formation or growth of nanoparticles. In summary, the reduction of gold ions in bulk water is spontaneous, and microdroplets are not essential, or the size of microdroplets is not the driving force for the spontaneity of this reduction reaction.

Since the formation of AuNPs from Au^{3+} is a reduction reaction, a parallel oxidation reaction must occur simultaneously. Therefore, to reveal the redox reaction's oxidation half-reaction, we performed solution-state NMR spectroscopy to investigate the possible oxidation products in a liquid state. Gas chromatography (GC) was performed to determine the evolution of the formed gases. NMR spectroscopy revealed the spontaneous formation of $\text{H}_2\text{O}_2(\text{aq})$ in the bulk HAuCl_4 solution, and GC revealed the gradual evolution of oxygen (O_2) gas in the headspace (Figs. 3a and S5). The formation of H_2O_2 was also observed and quantified using HPAK (Fig. 3b). The mechanistic insights into this chemistry are elaborated in the Discussion section.



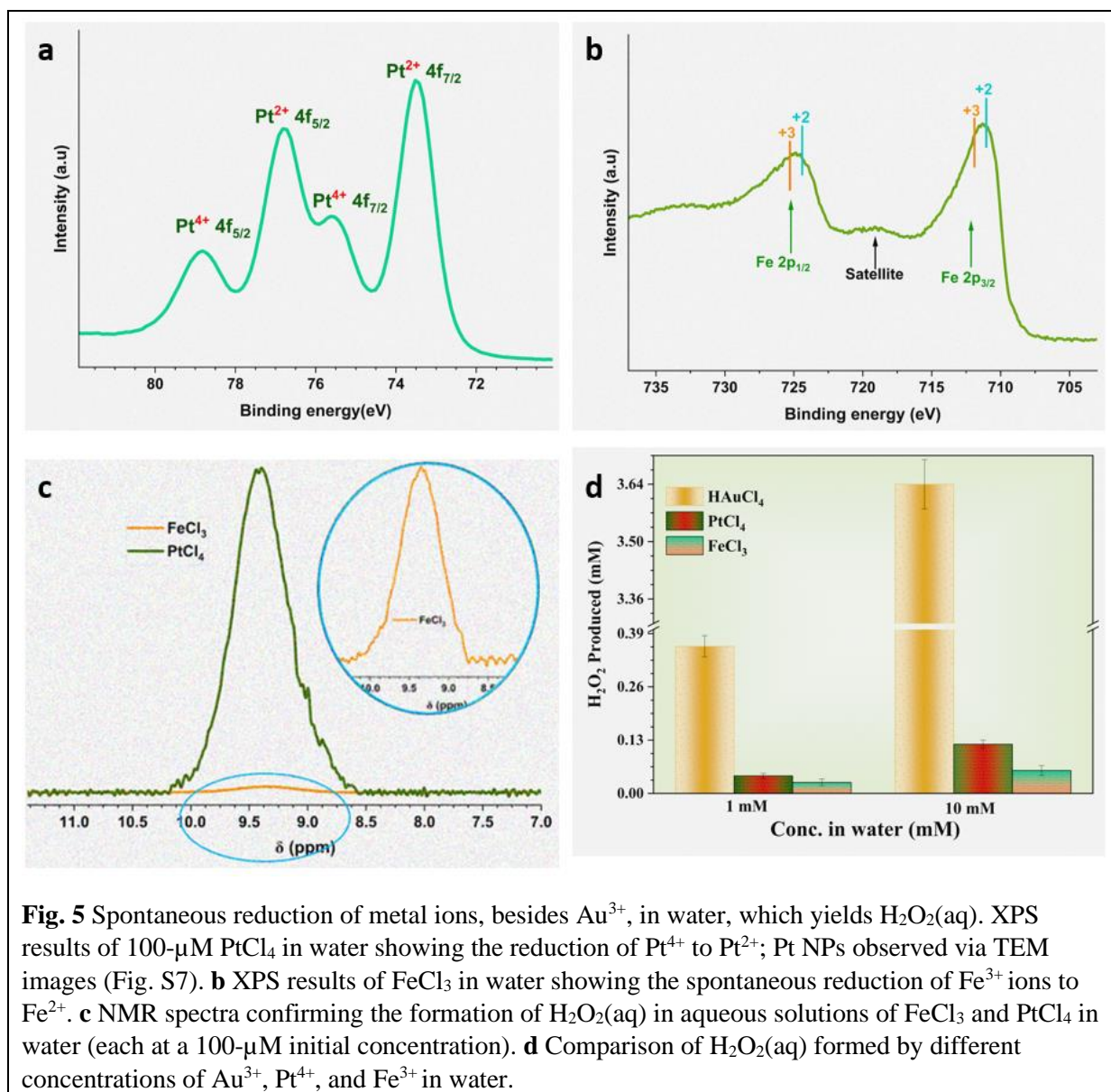
The concentration of $\text{H}_2\text{O}_2(\text{aq})$ formed spontaneously during the reduction of gold ions in bulk water increased with Au^{3+} concentration (Fig. 3b), possibly due to the oxidation of H_2O that produced H_2O_2 rather than the reduction of $\text{O}_2(\text{aq})$. $\text{H}_2\text{O}_2(\text{aq})$ formation in HAuCl_4 solutions prepared using water with dissolved oxygen and deoxygenated water was examined. We found that the dissolved oxygen had no measurable effect on H_2O_2 formation in aqueous HAuCl_4 solutions (Fig. S6). Thus, we confirmed the formation of $\text{H}_2\text{O}_2(\text{aq})$ from bulk water as the oxidation half-reaction occurring during the spontaneous formation of Au NPs.

Next, we investigated the effects of solution pH and concentration of Au^{3+} on the formation of AuNPs and corresponding H_2O_2 in water. As the solution turned acidic, the formation of the AuNPs and the corresponding production of H_2O_2 decreased (Fig. 4a–d). SEM imaging revealed that when a 200- μM HAuCl_4 solution was prepared using deionized water, 0.1-M HCl, or 1-M HCl, the nanoparticles were well-formed (Fig. 4b) or smaller and lesser (Fig. 4c), or nearly absent (Fig. 4d), respectively. This indicates that gold-ions are more stable at lower pH or highly acidic aqueous solutions. The effect of gold ion concentration on the formation of Au NPs and H_2O_2 was also examined. Results revealed that gold ions could undergo complete reduction to form Au NPs in relatively diluted solutions (<0.05 M), whereas in concentrated solutions (>0.05 M), Au^{3+} primarily reduced to lower oxidation states (mostly Au^{+1}). In both cases, H_2O_2 was produced stoichiometrically. XPS also revealed that as the salt concentration increased, the ratio of hydrated ions $\text{Au}^{1+}/\text{Au}^{3+}$ decreased (Fig. 4e).



To further elucidate whether the mechanisms underlying this chemical transformation, i.e., the spontaneous reduction of Au^{3+} in water, is unique or common with other metal ions, a few common metal ions such as Pt^{4+} , Al^{3+} , Fe^{3+} , Gd^{3+} , Fe^{2+} , Cu^{2+} , Mg^{2+} , Ni^{2+} , Zn^{2+} , and Na^{+}

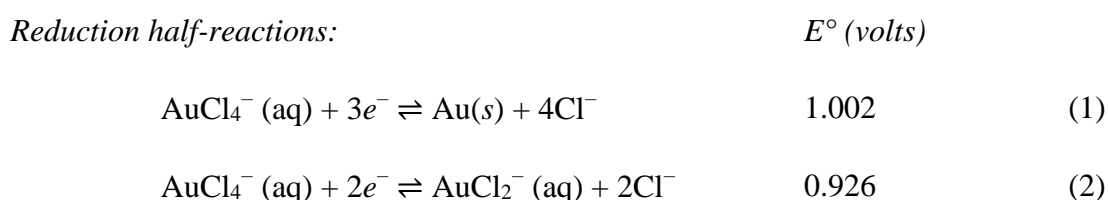
were also tested. The reduction of Au^{3+} in other solvents such as methanol, ethanol, and acetonitrile were studied to analyze the uniqueness of water or the air- water interface. We found that two metal cations, Pt^{4+} and Fe^{3+} , produced H_2O_2 in water (Fig. 5c,d), and the remaining cations did not produce H_2O_2 . Moreover, considerably higher amounts of H_2O_2 were produced by Au^{3+} reduction than those produced via Pt^{4+} and Fe^{3+} reduction.



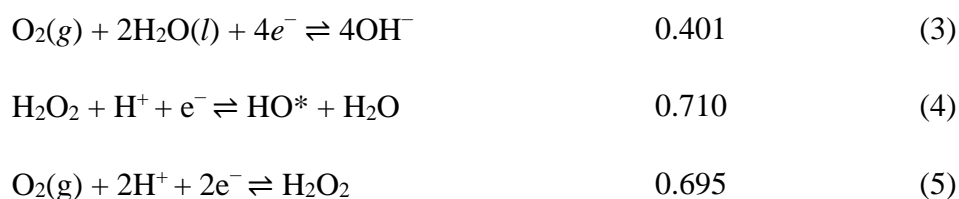
XPS analysis confirmed that Pt^{4+} and Fe^{3+} were spontaneously reduced in water similar to Au^{3+} , yielding Pt^{2+} and Fe^2 (Fig. 5a,b), and the formation of Pt NPs was observed by TEM imaging (Fig. S7). Notably, the reduction of Fe^{3+} to its zero-valent form was not observed. In other words, of all the metal ions studied herein, the pure metallic form of NPs was only observed in HAuCl_4 and PtCl_4 solutions.

Discussion

This section consolidates all the findings and presents mechanistic insights. We unambiguously established that the spontaneous reduction of Au^{3+} in water forms Au NPs and that this phenomenon is not limited to water microdroplets. This reduction reaction starts in the bulk solution right after its preparation. In fact, spraying bulk solutions and collecting the microdroplets reveals no significant enhancement in the size of AuNPs, suggesting that the microdroplet environment's effects, if any, are minor, such as facilitating solvent evaporation. Based on our experimental results, wherein Au^{3+} in bulk HAuCl_4 solutions spontaneously reduce to Au^+ ions and AuNPs and drive the formation of $\text{H}_2\text{O}_2(\text{aq})$ (Figs. 2, 3, and S5) and decrease in the solution pH, we suggest the following half-reactions⁴⁰:



Possible feasible oxidation half-reactions that may drive the above reduction reactions:



The standard reduction potentials of equations (1) and (2) are higher or nobler than those of equations (3) and (4); therefore, it is possible that hydroxyl ions ($\text{OH}^- (\text{aq})$) and H_2O may be oxidized to form $\text{H}_2\text{O}_2(\text{aq})$, which later decomposes/oxidizes gradually with time and forms $\text{O}_2(\text{g})$ (Eq. (5) further reducing gold ions.

The formation of Au NPs in common solvents such as alcohols and acetonitrile were also investigated. We observed that Au^{3+} rapidly reduced in methanol and ethanol than in bulk water (Fig. 6a,b), and it was negligible/sluggish in acetonitrile (Fig. 6a,b). In a complementary experiment, we quantified the amount of the reducing agent (standard hydrogen peroxide, 30%) required to completely reduce a fixed concentration of gold solution (0.1-M HAuCl_4) in methanol, water, and acetonitrile; the volume percent of H_2O_2 required were 0.4 ± 0.1 , 1.0 ± 0.2 , and 35 ± 1 , respectively. This indicates that Au NP formation is not unique to water. In a methanol solution containing dissolved HAuCl_4 , we observed that the formation of Au NPs was accompanied by the formation of H_2O_2 , methylal ($\text{CH}_3\text{OCH}_2\text{OCH}_3$), and dimethyl

ether (CH_3OCH_3) (Fig. S8). We did not investigate mechanisms underlying these chemical transformations.

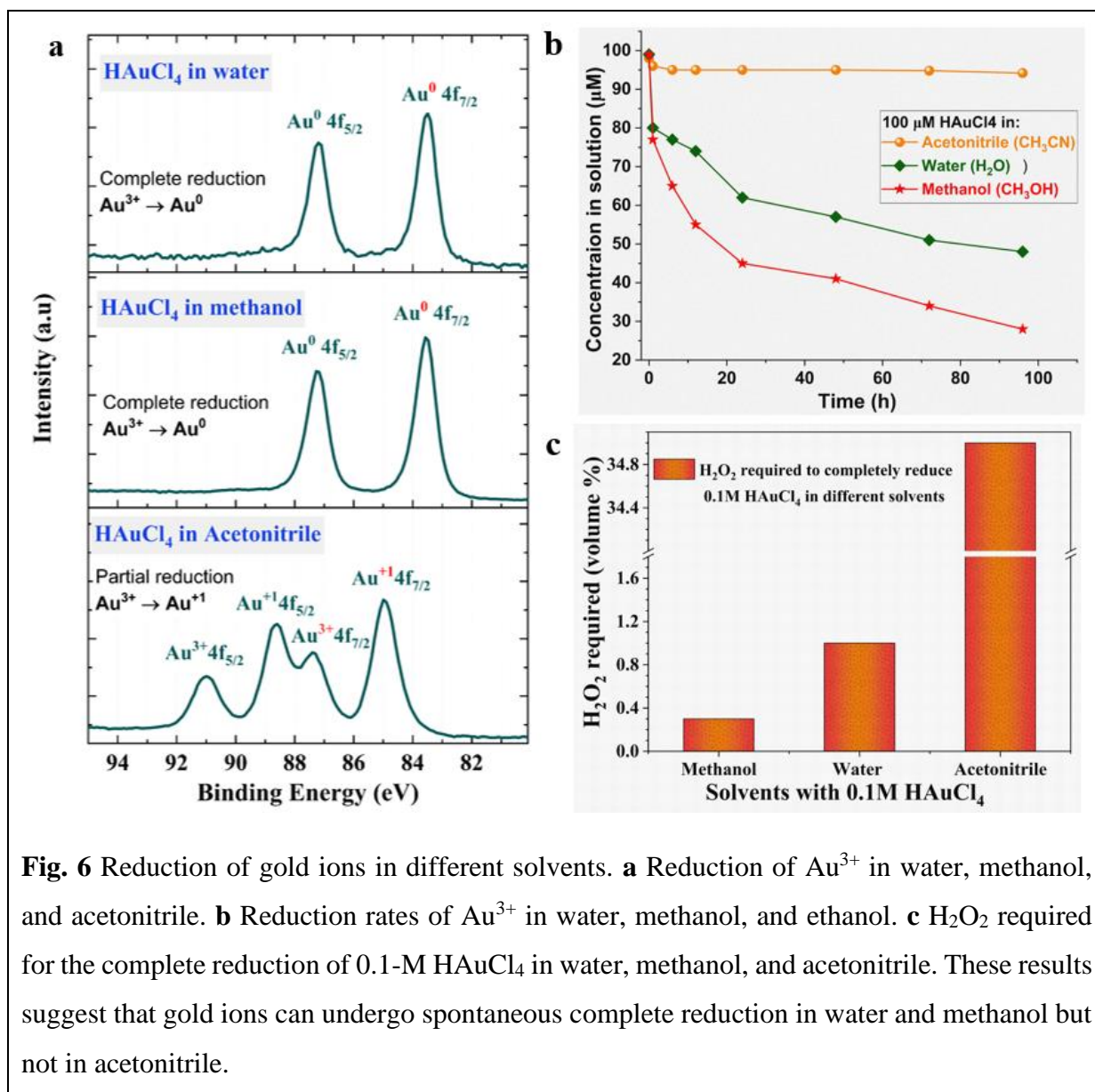


Fig. 6 Reduction of gold ions in different solvents. **a** Reduction of Au^{3+} in water, methanol, and acetonitrile. **b** Reduction rates of Au^{3+} in water, methanol, and ethanol. **c** H_2O_2 required for the complete reduction of 0.1-M HAuCl_4 in water, methanol, and acetonitrile. These results suggest that gold ions can undergo spontaneous complete reduction in water and methanol but not in acetonitrile.

Like gold cations, we probed the fate of Pt^{4+} in an aqueous PtCl_4 solution and Fe^{3+} in a $\text{FeCl}_3(\text{aq})$ solution. We found that $\text{Pt}^{4+}(\text{aq})$ was reduced to $\text{Pt}(\text{s})$ NPs and Pt^{2+} , whereas $\text{Fe}^{3+}(\text{aq})$ was reduced only to $\text{Fe}^{2+}(\text{aq})$ ions, and $\text{Fe}^0(\text{s})$ was not observed (Figs. 5 and S7). This was because the reduction potential of Pt^{4+} to $\text{Pt}(\text{s})$ and Pt^{2+} and that of Fe^{3+} ions to Fe^{2+} were nobler to water oxidation reactions (equations (3) and (4)) (Supplementary Table S2). As the reduction potentials of Fe^{3+} and Fe^{2+} to $\text{Fe}(\text{s})$ are -0.037 and -0.44 V, lower than those listed in equations (3) and (4), it is not feasible for Fe^{3+} or Fe^{2+} to reduce to $\text{Fe}(\text{s})$ by water. The reduction of Al^{3+} , Cu^{2+} , Ni^{2+} , Zn^{2+} , and Mg^{2+} in water also proceeds similarly (Supplementary Table S2).

Conclusions

In summary, our report refutes the claims that water microdroplets and the air–water interface has unique properties that enable the spontaneous reduction of gold ions. We demonstrated that this chemical transformation was not limited to (i) gold ions, (ii) water as a solvent, and (iii) microdroplets or the air–water interface. In other words, we confirmed that it was a bulk phenomenon. These findings are in alignment with our resolution of the latest controversy on the spontaneous formation of 0.3–1.5 μM of $\text{H}_2\text{O}_2(\text{aq})$ in water microdroplets, where we demonstrated that (i) microdroplets or the air–water interface has no bearing on the phenomenon (detection limit ≥ 50 nM) and (ii) the H_2O_2 formation was due to the reduction of dissolved $\text{O}_2(\text{aq})$ at the water–solid interface^{64, 73}. Essentially, the formation of AuNPs and $\text{H}_2\text{O}_2(\text{aq})$ in water can be explained simply by using the standard electrochemical series. The cations with very high reduction potential, such as Au^{3+} and Pt^{4+} , are so unstable that they can oxidize the solvent (water, methanol, and ethanol) to form NPs and $\text{H}_2\text{O}_2(\text{aq})$ (and other byproducts in the case of alcohols). In contrast, when metals with a high propensity for oxidation/corrosion, such as Mg and Al, contact water, they react with the dissolved $\text{O}_2(\text{aq})$ in water and form $\text{H}_2\text{O}_2(\text{aq})$. In the case of NP formation, the $\text{H}_2\text{O}_2(\text{aq})$ concentration is proportional to that of the metal salt. In contrast, in the case of surface oxidation of metals, the $\text{H}_2\text{O}_2(\text{aq})$ concentration is proportional to dissolved $\text{O}_2(\text{aq})$. These findings advance our understanding of aquatic chemistry and warrant caution in investigating microdroplet chemistry and its environmental and practical relevance.

Methods

Chemicals.

Gold(III) chloride trihydrate ($\text{HAuCl}_4 \cdot 3\text{H}_2\text{O}$, 520918), platinum(IV) chloride (PtCl_4 , 206113), iron(III) chloride hexahydrate ($\text{FeCl}_3 \cdot 6\text{H}_2\text{O}$, 10025-77-1), iron(II) chloride (FeCl_2 , 37287-0), aluminum(III) chloride (AlCl_3 , 06220), zinc chloride (ZnCl_2 , 211273), magnesium chloride hexahydrate ($\text{MgCl}_2 \cdot 6\text{H}_2\text{O}$, 13152), sodium chloride (NaCl , 7647145), ammonium chloride (NH_4Cl , 213330), and copper chloride (CuCl_2 , 7447394) were used. The following liquids were also used. Deuterium oxide (D_2O , 3000007892), methanol- D_4 +0.03%TMS, acetonitrile- D_3 (CAS 2206-26-0), acetonitrile (HPLC grade purchased from Fisher Scientific, batch 1072451), methanol (HPLC LC-MS grade), standard hydrogen peroxide (H_2O_2) 30% (Cat.270733), HPLC grade water (Cat. 2594649), and deionized water (DI) obtained from MilliQ Advantage 10 set up (with resistivity 18.2 $\text{M}\Omega \text{ cm}$).

Characterization of NPs

SEM and TEM analyses were performed to characterize the NPs in the bulk solutions. For SEM, a small drop of liquid containing NPs was drop-coated on a silicon wafer substrate, and the solution was dried at room temperature. TEM images were acquired using a Titan ST Image Corrected (Thermo Fisher) instrument operated at a 300-kV acceleration voltage. EDS spectra and maps were acquired in the STEM mode using a four-quadrant SuperX EDS detector. For sample preparation, a drop of solution was placed on an ultra-thin carbon-coated holey copper grid, blotted with filter paper, and dried under ambient conditions. The presence and growth of NPs were examined via DLS. The growth of Au NPs was observed in 100- μM HAuCl_4 bulk solution at varying time scales.

XPS measurements

For the XPS studies of gold ion reduction in water, 100- μM HAuCl_4 solution was used. The drop coating method was employed to prepare the samples using silicon wafers, and Baer's method was closely followed⁷⁴. Kratos Axis Supra instrument equipped with a monochromatic Al $\text{K}\alpha$ X-ray source ($h\nu = 1486.6 \text{ eV}$) operating at a power of 75 W and under UHV conditions in the range of $\sim 10^{-9}$ mbar was used to obtain the data. All the spectra were recorded in hybrid mode, using magnetic and electrostatic lenses and an aperture slot of $300 \mu\text{m} \times 700 \mu\text{m}$. The high-resolution spectra were acquired at fixed analyzer pass energies of 20 eV. The samples were mounted in a floating mode to avoid differential charging.

Quantification of H₂O₂

H₂O₂ concentration in all the diluted salt solutions was quantified using the hydrogen peroxide assay kit (HPAK). This is based on the principle that when hydrogen peroxide maintains contact with the AbIR peroxidase indicator, it causes fluorescence. Its maximum emission and excitation wavelengths are 674 and 647 nm, respectively. The samples were analyzed by mixing 50 μ L of HPAK reaction mixture with 50 μ L of samples in a 96-well black/transparent bottom microtiter plate using a SpectraMax M3 microplate reader. For the fluorescence reading, the SoftMax Pro 7 software was used. H₂O₂ in the samples was quantified using the calibration curve obtained from the standard samples on the same day.

Peroxide test strips for semi-quantitative analysis. For the qualitative estimation of H₂O₂ in the aqueous samples, peroxide test strips (Baker Test Strips purchased from VWR International) with a detection limit of 1 ppm were used. These strips use a colorimetric reagent that changes to blue when in contact with H₂O₂.

NMR spectroscopy for H₂O₂(aq) quantification

NMR measurements were performed on the 700 MHz Bruker Avance Neo NMR spectrometer equipped with a 5-mm Z-axis gradient TXO Cryoprobe at 275 K. For water samples, a 6-ms Gaussian 90-degree pulse was applied to excite the proton of hydrogen peroxide, followed by a 50-ms acquisition and a 1-ms recycle delay. For acetonitrile samples, a W5 binomial pulse sequence with gradients or a routine 1D proton pulse was applied for solvent suppression or nonsuppression measurements, respectively. Peak quantification and peak position confirmation of H₂O₂ in salt solutions were performed by comparing the results obtained for standard H₂O₂ samples.

GC-MS experiment

The methanol sample was extracted by adding 2 mL each of water and hexane to initiate phase separation. Approximately 1 μ L of the top hexane layer was analyzed using a single quadrupole GC-MS system (Agilent 7890 GC/5975C MSD) coupled to an EI source with an ionization energy of 70 eV. The ion source and mass analyzer temperatures were kept at 230 °C and 150 °C, respectively, with a solvent delay of 0 min. The mass analyzer was tuned according to the manufacturer's instructions, and the scan was fixed at 15–200 Da. A DB-5MS fused silica capillary column (30 m \times 0.25 mm I.D., 0.25- μ m film thickness; Agilent J&W Scientific, Folsom, CA) was used for chromatographic separation; the column contained a 5% phenyl and

95% methylpolysiloxane cross-linked stationary phase. Furthermore, helium was the carrier gas at a constant flow rate of 1.0 mL min⁻¹. The sample was injected into a 6890A gas chromatograph (Agilent, USA). The oven program was set to 30 °C and held for 10 min; the temperature was ramped at 20 °C/min to 260 °C with a 0-min hold time. The GC inlet temperature was set at 250 °C, and the transfer line temperature to the MS EI source was kept at 320 °C. The sample was injected using an autosampler equipped with a 10-μL syringe into a split/splitless inlet with a split ratio 10:1.

Oxygen gas analysis

Headspace analysis of the aqueous H₂AuCl₄ solution was performed using a gas analyzer (Model 310C, SRI, USA) equipped with a thermal conductivity detector (TCD). About 1 mL of the headspace above the sample was withdrawn using a gas-tight syringe (Hamilton, USA) and injected into a 6-foot molecular sieve 13X packed column. The oven temperature of the column was set to 100°C with argon as the carrier gas.

Acknowledgments

The co-authors thank Dr. Adair Gallo, Dr. Peng Zhong, and Ms. Nayara Musskopf for building a robust experimental setup in HM's laboratory; Dr. Ryo Mizuta, Scientific Illustrator at KAUST, for preparing illustrations in Fig. 1; Dr. Valentina-Elena Musteata, scientist from IAC at KAUST for her assistance with TEM; Mohammed Abdulwahab ElShaer from WDRC at Kaust for his assistance with DLS and Usman Sharif from Laboratory Equipment Maintenance (LEM) team at Kaust for his contribution to maintain the XPS instrument at the best operating conditions.

Author contributions: ME and HM designed the experiments, which ME performed. NK and ME performed LC-MS, GC, and ICP-OES experiments. XG and ME performed NMR spectroscopy experiments. NW and ME performed XPS studies. HM and ME wrote the manuscript.

Competing interests: The authors declare no competing interests.

Data and materials availability: All data needed to evaluate the conclusions in the paper are present in the paper or the Supplementary Materials.

Funding: HM acknowledges KAUST for funding (Grant No. BAS/1/1070-01-01).

References

- (1) Bruce Alberts, R. H., Alexander Johnson, David Morgan, Martin Raff, Keith Roberts, Peter Walter *Molecular Biology of the Cell (Seventh Edition)*; W. W. Norton & Company, 2022.
- (2) Rob Phillips, J. K., Julie Theriot, Hernan Garcia. *Physical Biology of the Cell* Garland Science, 2012.
- (3) Mark E. Davis, R. J. D. *Fundamentals of Chemical Reaction Engineering* Dover Publications, 2013.
- (4) Bal, W.; Kurowska, E.; Maret, W. The Final Frontier of pH and the Undiscovered Country Beyond. *PLOS ONE* **2012**, 7 (9), e45832. DOI: 10.1371/journal.pone.0045832.
- (5) Ruiz-Lopez, M. F.; Francisco, J. S.; Martins-Costa, M. T. C.; Anglada, J. M. Molecular reactions at aqueous interfaces. *Nature Reviews Chemistry* **2020**, 4 (9), 459-475. DOI: 10.1038/s41570-020-0203-2.
- (6) Stuve, E. M. Ionization of water in interfacial electric fields: An electrochemical view. *Chemical Physics Letters* **2012**, 519-520, 1-17. DOI: <https://doi.org/10.1016/j.cplett.2011.09.040>.
- (7) Ball, P. Water as an Active Constituent in Cell Biology. *Chemical Reviews* **2008**, 108 (1), 74-108. DOI: 10.1021/cr068037a.
- (8) Ahmed, M.; Blum, M.; Crumlin, E. J.; Geissler, P. L.; Head-Gordon, T.; Limmer, D. T.; Mandadapu, K. K.; Saykally, R. J.; Wilson, K. R. Molecular Properties and Chemical Transformations Near Interfaces. *The Journal of Physical Chemistry B* **2021**. DOI: 10.1021/acs.jpcb.1c03756.
- (9) Bonn, M. Concluding remarks for Faraday Discussion on Water at Interfaces. *Faraday Discussions* **2024**, 249 (0), 521-525, 10.1039/D3FD00153A. DOI: 10.1039/D3FD00153A.
- (10) Agmon, N.; Bakker, H. J.; Campen, R. K.; Henchman, R. H.; Pohl, P.; Roke, S.; Thämer, M.; Hassanali, A. Protons and Hydroxide Ions in Aqueous Systems. *Chemical Reviews* **2016**, 116 (13), 7642-7672. DOI: 10.1021/acs.chemrev.5b00736.
- (11) McCaffrey, D. L.; Nguyen, S. C.; Cox, S. J.; Weller, H.; Alivisatos, A. P.; Geissler, P. L.; Saykally, R. J. Mechanism of ion adsorption to aqueous interfaces: Graphene/water vs. air/water. *Proceedings of the National Academy of Sciences* **2017**. DOI: 10.1073/pnas.1702760114.
- (12) Pullanchery, S.; Kulik, S.; Rehl, B.; Hassanali, A.; Roke, S. Charge transfer across C–H···O hydrogen bonds stabilizes oil droplets in water. *Science* **2021**, 374 (6573), 1366-1370. DOI: doi:10.1126/science.abj3007.
- (13) Poli, E.; Jong, K. H.; Hassanali, A. Charge transfer as a ubiquitous mechanism in determining the negative charge at hydrophobic interfaces. *Nature Communications* **2020**, 11 (1), 901. DOI: 10.1038/s41467-020-14659-5.

- (14) Nauruzbayeva, J.; Sun, Z.; Gallo, A.; Ibrahim, M.; Santamarina, J. C.; Mishra, H. Electrification at water–hydrophobe interfaces. *Nature Communications* **2020**, *11* (1), 5285. DOI: 10.1038/s41467-020-19054-8.
- (15) Devlin, Shane W.; Bernal, F.; Riffe, E. J.; Wilson, K. R.; Saykally, R. J. Spiers Memorial Lecture: Water at interfaces. *Faraday Discussions* **2024**, *249* (0), 9-37, 10.1039/D3FD00147D. DOI: 10.1039/D3FD00147D.
- (16) Nam, I.; Nam, H. G.; Zare, R. N. Abiotic synthesis of purine and pyrimidine ribonucleosides in aqueous microdroplets. *Proceedings of the National Academy of Sciences* **2018**, *115* (1), 36. DOI: 10.1073/pnas.1718559115.
- (17) Banerjee, S.; Gnanamani, E.; Yan, X.; Zare, R. N. Can all bulk-phase reactions be accelerated in microdroplets? *Analyst* **2017**, *142* (9), 1399-1402, 10.1039/C6AN02225A. DOI: 10.1039/C6AN02225A.
- (18) Huang, K.-H.; Morato, N. M.; Feng, Y.; Cooks, R. G. High-throughput Diversification of Complex Bioactive Molecules by Accelerated Synthesis in Microdroplets. *Angewandte Chemie International Edition* **2023**, *n/a* (n/a), e202300956, <https://doi.org/10.1002/anie.202300956>. DOI: <https://doi.org/10.1002/anie.202300956> (accessed 2023/03/28).
- (19) Holden, D. T.; Morato, N. M.; Cooks, R. G. Aqueous microdroplets enable abiotic synthesis and chain extension of unique peptide isomers from free amino acids. *Proceedings of the National Academy of Sciences* **2022**, *119* (42), e2212642119. DOI: 10.1073/pnas.2212642119 (accessed 2023/03/28).
- (20) Rovelli, G.; Jacobs, M. I.; Willis, M. D.; Rapf, R. J.; Prophet, A. M.; Wilson, K. R. A critical analysis of electrospray techniques for the determination of accelerated rates and mechanisms of chemical reactions in droplets. *Chemical Science* **2020**, *11* (48), 13026-13043, 10.1039/D0SC04611F. DOI: 10.1039/D0SC04611F.
- (21) Nguyen, D.; Casillas, S.; Vang, H.; Garcia, A.; Mizuno, H.; Riffe, E. J.; Saykally, R. J.; Nguyen, S. C. Catalytic Mechanism of Interfacial Water in the Cycloaddition of Quadricyclane and Diethyl Azodicarboxylate. *The Journal of Physical Chemistry Letters* **2021**, *12* (12), 3026-3030. DOI: 10.1021/acs.jpclett.1c00565.
- (22) Griffith, E. C.; Vaida, V. In situ observation of peptide bond formation at the water–air interface. *Proceedings of the National Academy of Sciences* **2012**, *109* (39), 15697-15701. DOI: 10.1073/pnas.1210029109.
- (23) Wei, Z.; Li, Y.; Cooks, R. G.; Yan, X. Accelerated Reaction Kinetics in Microdroplets: Overview and Recent Developments. *Annual Review of Physical Chemistry* **2020**, *71* (Volume 71, 2020), 31-51. DOI: <https://doi.org/10.1146/annurev-physchem-121319-110654>.
- (24) Qiu, L.; Cooks, R. G. Spontaneous Oxidation in Aqueous Microdroplets: Water Radical Cation as Primary Oxidizing Agent. *Angewandte Chemie International Edition* **2024**, *n/a* (n/a), e202400118. DOI: <https://doi.org/10.1002/anie.202400118> (accessed 2024/04/09).

- (25) Ruiz-Lopez, M. F. Midair transformations of aerosols. *Science* **2021**, 374 (6568), 686-687. DOI: 10.1126/science.abl8914 (accessed 2024/04/09).
- (26) Schiffer, J. M.; Mael, L. E.; Prather, K. A.; Amaro, R. E.; Grassian, V. H. Sea Spray Aerosol: Where Marine Biology Meets Atmospheric Chemistry. *ACS Central Science* **2018**, 4 (12), 1617-1623. DOI: 10.1021/acscentsci.8b00674.
- (27) Mofidfar, M.; Mehrgardi, M. A.; Xia, Y.; Zare, R. N. Dependence on relative humidity in the formation of reactive oxygen species in water droplets. *Proceedings of the National Academy of Sciences* **2024**, 121 (12), e2315940121. DOI: 10.1073/pnas.2315940121 (accessed 2024/04/09).
- (28) Stadnytskyi, V.; Anfinrud, P.; Bax, A. Breathing, speaking, coughing or sneezing: What drives transmission of SARS-CoV-2? *Journal of Internal Medicine* **2021**, 290 (5), 1010-1027. DOI: <https://doi.org/10.1111/joim.13326> (accessed 2024/04/09).
- (29) Vaida, V. Prebiotic phosphorylation enabled by microdroplets. *Proceedings of the National Academy of Sciences* **2017**, 114 (47), 12359-12361. DOI: 10.1073/pnas.1717373114.
- (30) Seinfeld, J. H.; Pandis, S. N. *Atmospheric Chemistry and Physics: From Air Pollution to Climate Change*; Wiley-Interscience; 2 edition (August 11, 2006), 1998.
- (31) Pruppacher, H. R.; Klett, J. D. *Microphysics of Clouds and Precipitation*; D. Reidel Publishing Company, 1980.
- (32) Mishra, H.; Nielsen, R. J.; Enami, S.; Hoffmann, M. R.; Colussi, A. J.; Goddard, W. A. Quantum chemical insights into the dissociation of nitric acid on the surface of aqueous electrolytes. *International Journal of Quantum Chemistry* **2013**, 113 (4), 413-417.
- (33) Hillel, D. *Introduction to Soil Physics*; Academic Press, 1982.
- (34) Otter, J. A.; Yezli, S.; Barbut, F.; Perl, T. M. An overview of automated room disinfection systems: When to use them and how to choose them. *Decontamination in Hospitals and Healthcare* **2020**, 323-369. DOI: 10.1016/B978-0-08-102565-9.00015-7 PMC.
- (35) Pillai, S.; Santana, A.; Das, R.; Shrestha, B. R.; Manalastas, E.; Mishra, H. A molecular to macro level assessment of direct contact membrane distillation for separating organics from water. *Journal of Membrane Science* **2020**, 608, 118140. DOI: <https://doi.org/10.1016/j.memsci.2020.118140>.
- (36) Benjamin, M. M. *Water Chemistry*; Waveland Press, Inc., 2015.
- (37) Garcia-Ochoa, F.; Gomez, E. Bioreactor scale-up and oxygen transfer rate in microbial processes: an overview. *Biotechnology advances* **2009**, 27 (2), 153-176.
- (38) Ali, M.; Hong, P.-Y.; Mishra, H.; Vrouwenvelder, J.; Saikaly, P. E. Adopting the circular model: opportunities and challenges of transforming wastewater treatment plants into resource recovery factories in Saudi Arabia. *Water Reuse* **2022**, 12 (3), 346-365. DOI: 10.2166/wrd.2022.038 (accessed 3/28/2023).

- (39) Santana, A.; Farinha, A. S. F.; Torano, A. Z.; Ibrahim, M.; Mishra, H. First-Principles Based Rationally Designed Materials for the Removal of Methylene Blue from Wastewaters. (*Under review in The Journal of Physical Chemistry C*) **2019**.
- (40) Bard, A. J.; Faulkner, L. R. *Electrochemical Methods: Fundamentals and Applications*; John Wiley & Sons, 2001.
- (41) Mishra, H.; Cola, B. A.; Rawat, V.; Amama, P. B.; Biswas, K. G.; Xu, X. F.; Fisher, T. S.; Sands, T. D. Thermomechanical and Thermal Contact Characteristics of Bismuth Telluride Films Electrodeposited on Carbon Nanotube Arrays. *Advanced Materials* **2009**, *21* (42), 4280-+. DOI: 10.1002/adma.200803705.
- (42) De Hoffmann, E.; Stroobant, V. *Mass spectrometry: principles and applications*; John Wiley & Sons, 2007.
- (43) Ingram, A. J.; Boeser, C. L.; Zare, R. N. Going beyond electrospray: mass spectrometric studies of chemical reactions in and on liquids. *Chemical Science* **2016**, *7* (1), 39-55. DOI: 10.1039/c5sc02740c.
- (44) Enami, S.; Mishra, H.; Hoffmann, M. R.; Colussi, A. J. Protonation and Oligomerization of Gaseous Isoprene on Mildly Acidic Surfaces: Implications for Atmospheric Chemistry. *J Phys Chem A* **2012**, *116* (24), 6027-6032. DOI: Doi 10.1021/Jp2110133.
- (45) Colussi, A. J.; Enami, S.; Ishizuka, S. Hydronium Ion Acidity Above and Below the Interface of Aqueous Microdroplets. *ACS Earth and Space Chemistry* **2021**, *5* (9), 2341-2346. DOI: 10.1021/acsearthspacechem.1c00067.
- (46) Gallo, A.; Farinha, A. S. F.; Dinis, M.; Emwas, A.-H.; Santana, A.; Nielsen, R. J.; Goddard, W. A.; Mishra, H. The chemical reactions in electrosprays of water do not always correspond to those at the pristine air–water interface. *Chemical Science* **2019**, *10* (9), 2566-2577, 10.1039/C8SC05538F. DOI: 10.1039/C8SC05538F.
- (47) Colussi, A. J.; Enami, S. Comment on “The chemical reactions in electrosprays of water do not always correspond to those at the pristine air–water interface” by A. Gallo Jr, A. S. F. Farinha, M. Dinis, A.-H. Emwas, A. Santana, R. J. Nielsen, W. A. Goddard III and H. Mishra, *Chem. Sci.*, 2019, 10, 2566. *Chemical Science* **2019**, 10.1039/C9SC00991D. DOI: 10.1039/C9SC00991D.
- (48) Gallo, A.; Farinha, A. S. F.; Emwas, A.-H.; Santana, A.; Nielsen, R. J.; Goddard, W. A.; Mishra, H. Reply to the ‘Comment on “The chemical reactions in electrosprays of water do not always correspond to those at the pristine air–water interface”’ by A. J. Colussi and S. Enami, *Chem. Sci.*, 2019, 10, DOI: 10.1039/c9sc00991d. *Chemical Science* **2019**, 10.1039/C9SC02702E. DOI: 10.1039/C9SC02702E.
- (49) Jacobs, M. I.; Davis, R. D.; Rapf, R. J.; Wilson, K. R. Studying Chemistry in Micro-compartments by Separating Droplet Generation from Ionization. *Journal of The American Society for Mass Spectrometry* **2019**, *30* (2), 339-343. DOI: 10.1007/s13361-018-2091-y.

- (50) Martins-Costa, M. T.; Ruiz-López, M. F. Probing solvation electrostatics at the air–water interface. *Theoretical Chemistry Accounts* **2023**, *142* (3), 29.
- (51) Wilson, K. R.; Prophet, A. M. Chemical Kinetics in Microdroplets. *Annual Review of Physical Chemistry* **2024**. DOI: <https://doi.org/10.1146/annurev-physchem-052623-120718>.
- (52) Lee, J. K.; Walker, K. L.; Han, H. S.; Kang, J.; Prinz, F. B.; Waymouth, R. M.; Nam, H. G.; Zare, R. N. Spontaneous generation of hydrogen peroxide from aqueous microdroplets. *Proceedings of the National Academy of Sciences of the United States of America* **2019**, *116* (39), 19294-19298. DOI: 10.1073/pnas.1911883116.
- (53) Dulay, M. T.; Huerta-Aguilar, C. A.; Chamberlayne, C. F.; Zare, R. N.; Davidse, A.; Vukovic, S. Effect of relative humidity on hydrogen peroxide production in water droplets. *QRB Discovery* **2021**, *2*, e8. DOI: 10.1017/qrd.2021.6 From Cambridge University Press Cambridge Core.
- (54) Lee, J. K.; Han, H. S.; Chaikasetin, S.; Marron, D. P.; Waymouth, R. M.; Prinz, F. B.; Zare, R. N. Condensing water vapor to droplets generates hydrogen peroxide. *Proceedings of the National Academy of Sciences of the United States of America* **2020**, *117* (49), 30934-30941. DOI: 10.1073/pnas.2020158117.
- (55) Mehrgardi, M. A.; Mofidfar, M.; Zare, R. N. Sprayed Water Microdroplets Are Able to Generate Hydrogen Peroxide Spontaneously. *Journal of the American Chemical Society* **2022**, *144* (17), 7606-7609. DOI: 10.1021/jacs.2c02890.
- (56) Heindel, J. P.; Hao, H.; LaCour, R. A.; Head-Gordon, T. Spontaneous formation of hydrogen peroxide in water microdroplets. *The Journal of Physical Chemistry Letters* **2022**, *13* (43), 10035-10041.
- (57) Hao, H.; Leven, I.; Head-Gordon, T. Can electric fields drive chemistry for an aqueous microdroplet? *Nature communications* **2022**, *13* (1), 280.
- (58) Ben-Amotz, D. Electric buzz in a glass of pure water. *Science* **2022**, *376* (6595), 800-801. DOI: 10.1126/science.abo3398 (accessed 2023/11/15).
- (59) Colussi, A. J. Mechanism of Hydrogen Peroxide Formation on Sprayed Water Microdroplets. *Journal of the American Chemical Society* **2023**, *145* (30), 16315-16317. DOI: 10.1021/jacs.3c04643.
- (60) Gallo Jr, A.; Muskopf, N. H.; Liu, X.; Yang, Z.; Petry, J.; Zhang, P.; Thoroddsen, S.; Im, H.; Mishra, H. On the formation of hydrogen peroxide in water microdroplets. *Chemical Science* **2022**, *13* (9), 2574-2583, 10.1039/D1SC06465G. DOI: 10.1039/D1SC06465G.
- (61) Muskopf, N. H.; Gallo, A.; Zhang, P.; Petry, J.; Mishra, H. The Air–Water Interface of Water Microdroplets Formed by Ultrasonication or Condensation Does Not Produce H₂O₂. *The Journal of Physical Chemistry Letters* **2021**, *12* (46), 11422-11429. DOI: 10.1021/acs.jpcllett.1c02953.

- (62) Peplow, M. Claims of water turning into hydrogen peroxide spark debate. In *C&EN*, American Chemical Society: 2022.
- (63) Cozens, T. Study casts doubt on water microdroplets' ability to spontaneously produce hydrogen peroxide. In *Chemistry World*, Royal Society of Chemistry: 2022.
- (64) Eatoo, M. A.; Mishra, H. Busting the myth of spontaneous formation of H₂O₂ at the air–water interface: contributions of the liquid–solid interface and dissolved oxygen exposed. *Chemical Science* **2024**, *15* (9), 3093-3103, 10.1039/D3SC06534K. DOI: 10.1039/D3SC06534K.
- (65) Chen, B.; Xia, Y.; He, R.; Sang, H.; Zhang, W.; Li, J.; Chen, L.; Wang, P.; Guo, S.; Yin, Y.; et al. Water–solid contact electrification causes hydrogen peroxide production from hydroxyl radical recombination in sprayed microdroplets. *Proceedings of the National Academy of Sciences* **2022**, *119* (32), e2209056119. DOI: doi:10.1073/pnas.2209056119.
- (66) Dulay, M. T.; Lee, J. K.; Mody, A. C.; Narasimhan, R.; Monack, D. M.; Zare, R. N. Spraying Small Water Droplets Acts as a Bacteriocide. *QRB Discovery* **2020**, *1*, e3. DOI: 10.1017/qrd.2020.2 From Cambridge University Press Cambridge Core.
- (67) Nguyen, D.; Nguyen, S. C. Revisiting the Effect of the Air–Water Interface of Ultrasonically Atomized Water Microdroplets on H₂O₂ Formation. *The Journal of Physical Chemistry B* **2022**, *126* (16), 3180-3185. DOI: 10.1021/acs.jpcc.2c01310.
- (68) Koppenol, W. H.; Sies, H. Was hydrogen peroxide present before the arrival of oxygenic photosynthesis? The important role of iron(II) in the Archean ocean. *Redox Biology* **2024**, *69*, 103012. DOI: <https://doi.org/10.1016/j.redox.2023.103012>.
- (69) Lee, J. K.; Samanta, D.; Nam, H. G.; Zare, R. N. Spontaneous formation of gold nanostructures in aqueous microdroplets. *Nature Communications* **2018**, *9* (1), 1562. DOI: 10.1038/s41467-018-04023-z.
- (70) Liu, Z.; Yu, R.; Wang, X.; Chen, Q. The reducing role of hydrogen peroxide on the formation of gold nanostructures in aqueous microdroplets with dissolved tetrachloroaurate ions. 2021.
- (71) Gutiérrez-Wing, C.; Esparza, R.; Vargas-Hernández, C.; Fernández García, M. E.; José-Yacamán, M. Microwave-assisted synthesis of gold nanoparticles self-assembled into self-supported superstructures. *Nanoscale* **2012**, *4* (7), 2281-2287. DOI: 10.1039/c2nr12053d From NLM.
- (72) Graedel, T. E.; Weschler, C. J.; Mandich, M. L. Influence of transition metal complexes on atmospheric droplet acidity. *Nature* **1985**, *317* (6034), 240-242. DOI: 10.1038/317240a0.
- (73) Trager, R. Water surprise: microdroplets have potential to produce hydrogen peroxide. In *Chemistry World*, Royal Society of Chemistry: 2019.
- (74) Baer, D. R. Guide to making XPS measurements on nanoparticles. *J Vac Sci Technol A* **2020**, *38* (3). DOI: Artn 031201

10.1116/1.5141419.

Supplementary Information

Why Some Metal Ions Spontaneously Form Nanoparticles in Water Microdroplets: Disentangling the Contributions of the Air–Water Interface and Bulk Redox Chemistry

Muzzamil Ahmad Eatoo^{a,b,c,d}, Nimer Wehbe^e, Najeh Kharbatia^b, Xianrong Guo^e, Himanshu Mishra^{a,b,c,d*}

^aEnvironmental Science and Engineering (EnSE) Program, Biological and Environmental Science and Engineering (BESE) Division, Water Desalination and Reuse Center (WDRC)

^bWater Desalination and Reuse Center (WDRC),

King Abdullah University of Science and Technology (KAUST), Thuwal, 23955-6900,
Kingdom of Saudi Arabia

^cCenter for Desert Agriculture (CDA), King Abdullah University of Science and Technology (KAUST), Thuwal 23955-6900, Saudi Arabia

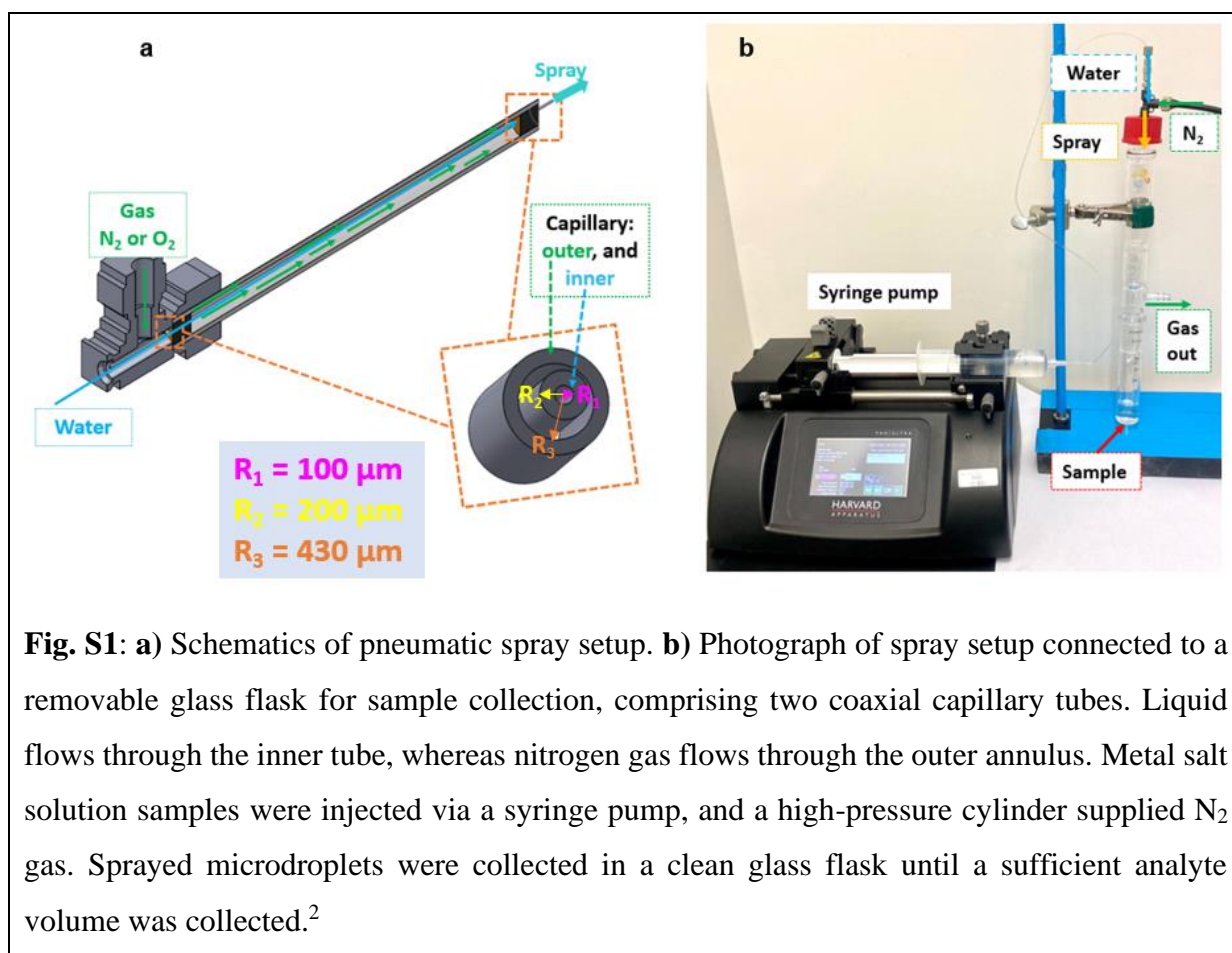
^dInterfacial Lab (iLab), King Abdullah University of Science and Technology (KAUST),
Thuwal 23955-6900, Saudi Arabia

^eCore Labs, King Abdullah University of Science and Technology (KAUST), Thuwal 23955-6900, Saudi Arabia

*Correspondence: himanshu.mishra@kaust.edu.sa

Section S1: Water microdroplet generation via sprays

We adapted the experimental setup built by Gallo et al.¹ to produce water microdroplets. In a coaxial system, water was injected through an inner tube with a 100- μm diameter using a syringe pump (PHD Ultra, Harvard Apparatus). Dry $\text{N}_2(\text{g})$ was pushed through the outer tube with a 430- μm diameter. Additionally, HPLC-grade water was used to make salt solutions, and a glass cell (equipped with a tiny opening to prevent pressure build-up) was employed to collect microdroplets while minimizing ambient contamination. The water flow rate was 25 $\mu\text{L}/\text{min}$, whereas the gas (N_2) pressure was 100 psi.



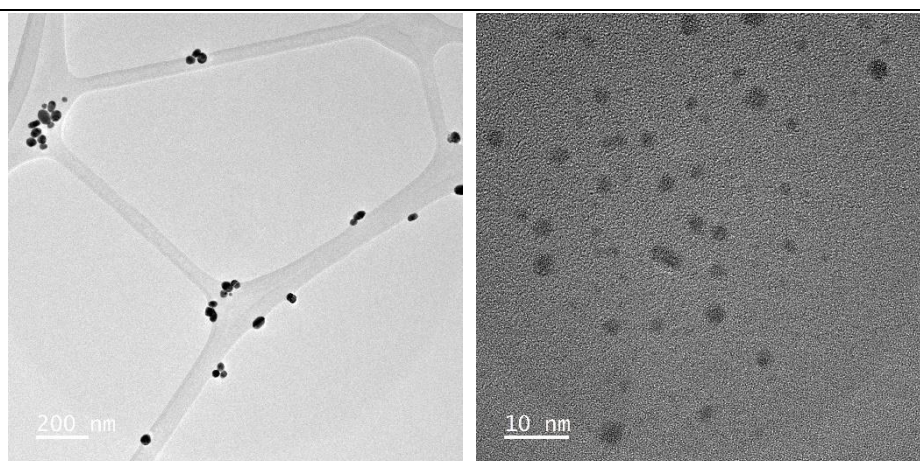


Fig. S2 TEM imaging of microdroplets samples formed by spraying 100 μM HAuCl_4 solution, collected and drop cast, shows the presence of AuNPs.

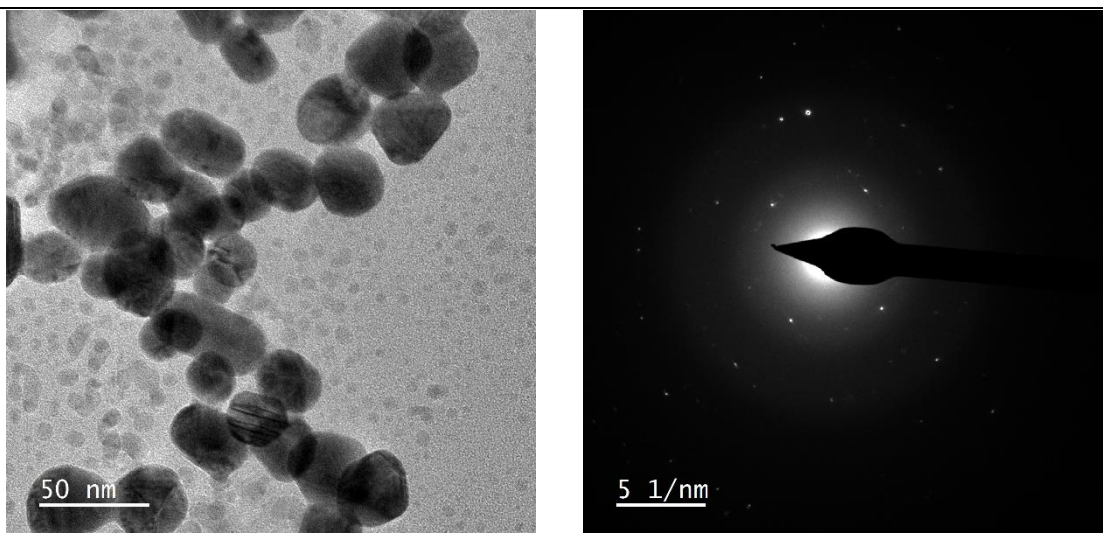


Fig. S3 TEM imaging of bulk aqueous 100 μM HAuCl_4 solution: Micrograph showing the presence of nanoparticles of different sizes and diffraction pattern showing the formation of $\text{Au}(0)$.

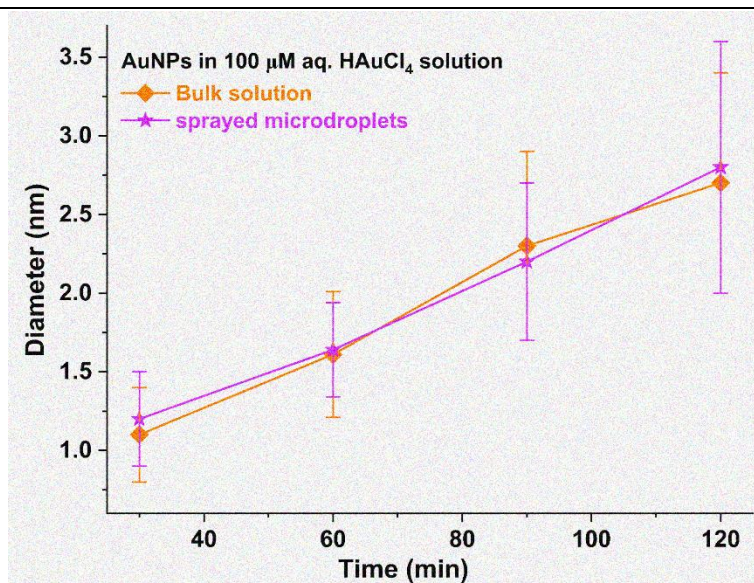


Fig. S4 shows DLS measurements for the growth kinetics of nanoparticles in microdroplets vs. bulk solution.

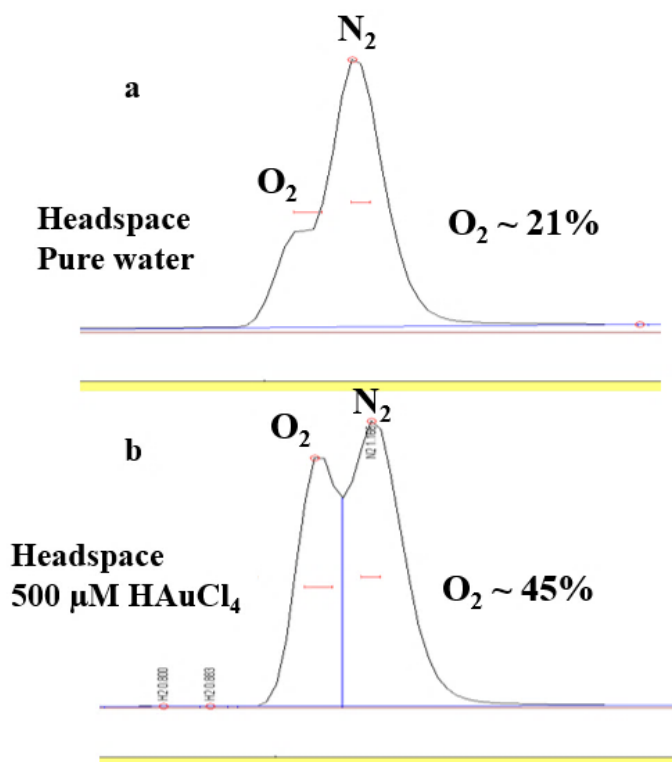


Fig. S5: Gas chromatography results show oxygen gas evolution from the HAuCl₄ aqueous solution. **a** showing the presence of around 21% oxygen in the headspace of pure water (DI used for making solutions). **b** shows the presence of around 45% oxygen in the headspace of 500 μM HAuCl₄ solution after the age of around 24 h. This reveals that the HAuCl₄ solution evolves oxygen gas.

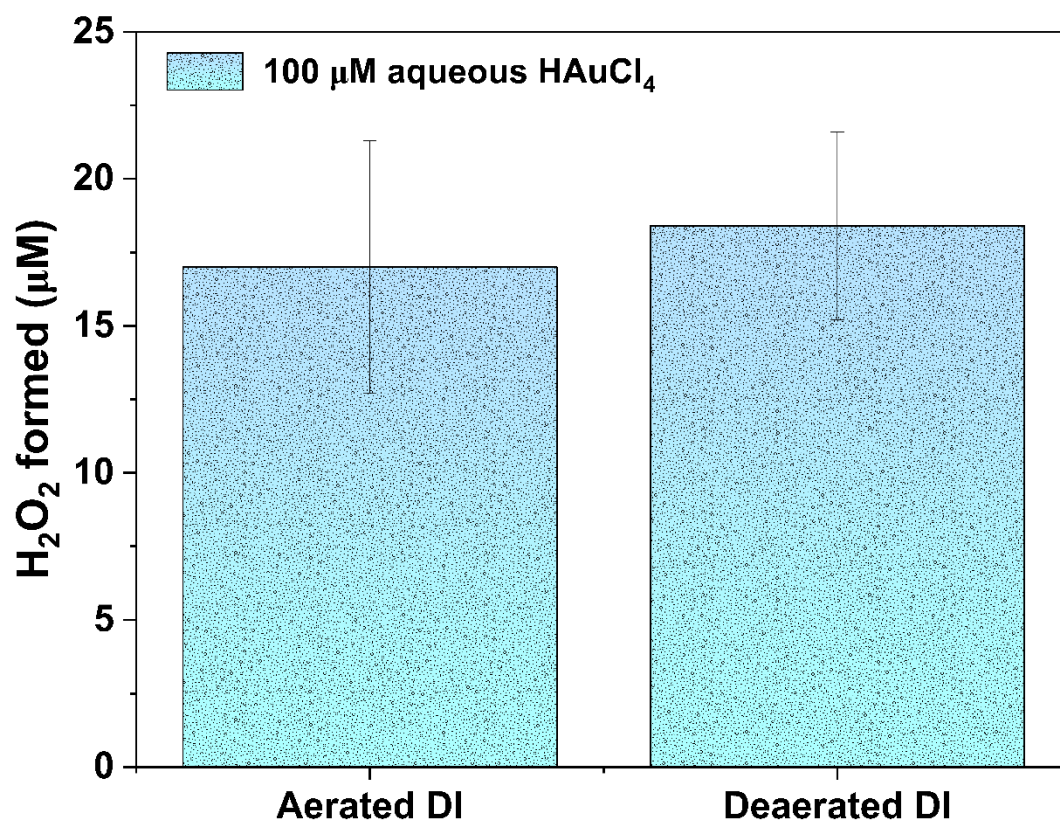


Fig. S6 Effect of water deaeration on H_2O_2 formation by Au^{3+} cations in water. These results reveal that deaeration has no significant effect on the H_2O_2 formation.

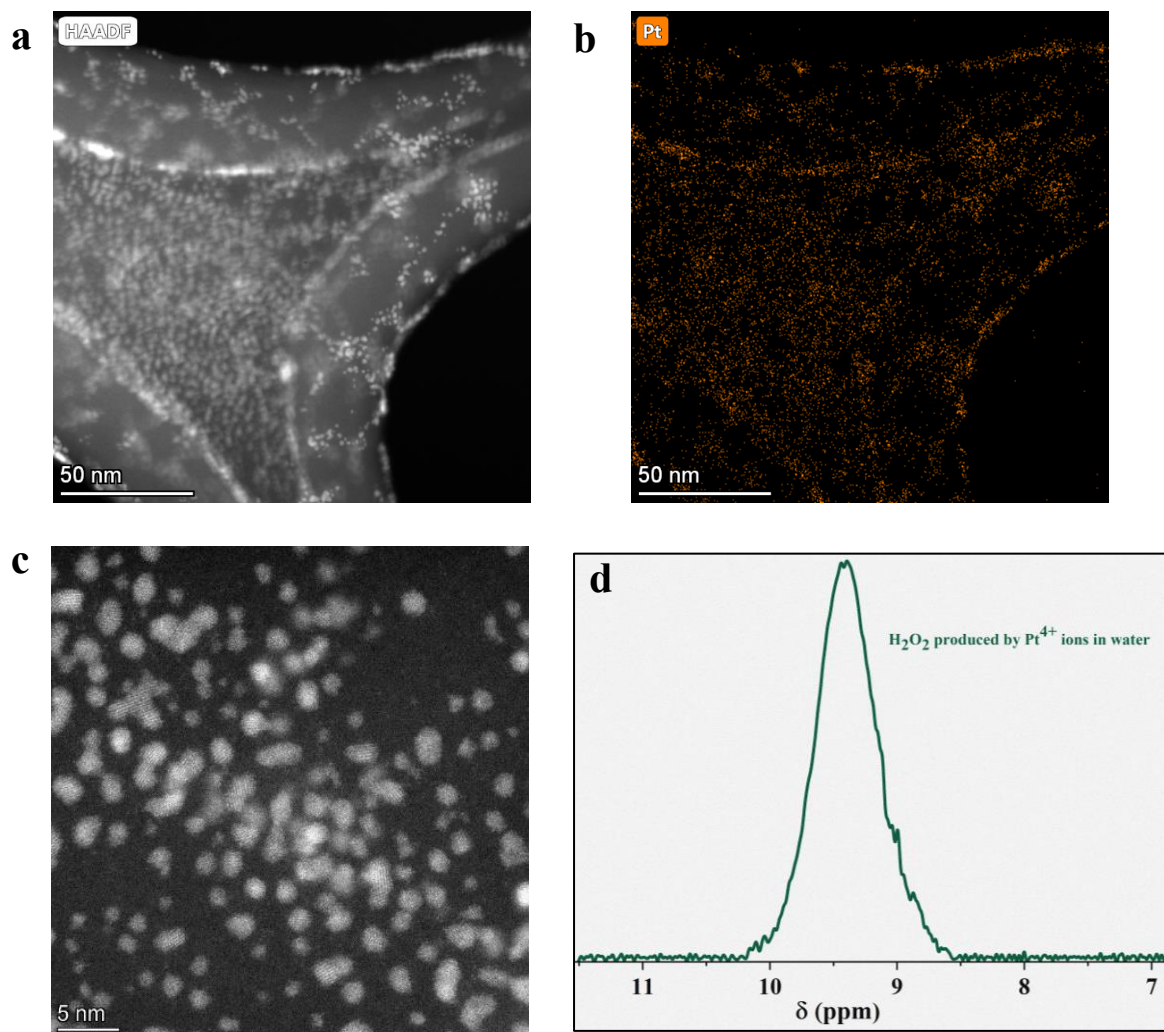


Fig. S7 Characterization of bulk aqueous PtCl₄ solution. **a-c** TEM imaging of drop casted bulk PtCl₄ solution shows the presence of Pt nanoparticles. **d** NMR spectroscopy results revealing H₂O₂ formation by Pt⁴⁺ ions in water.

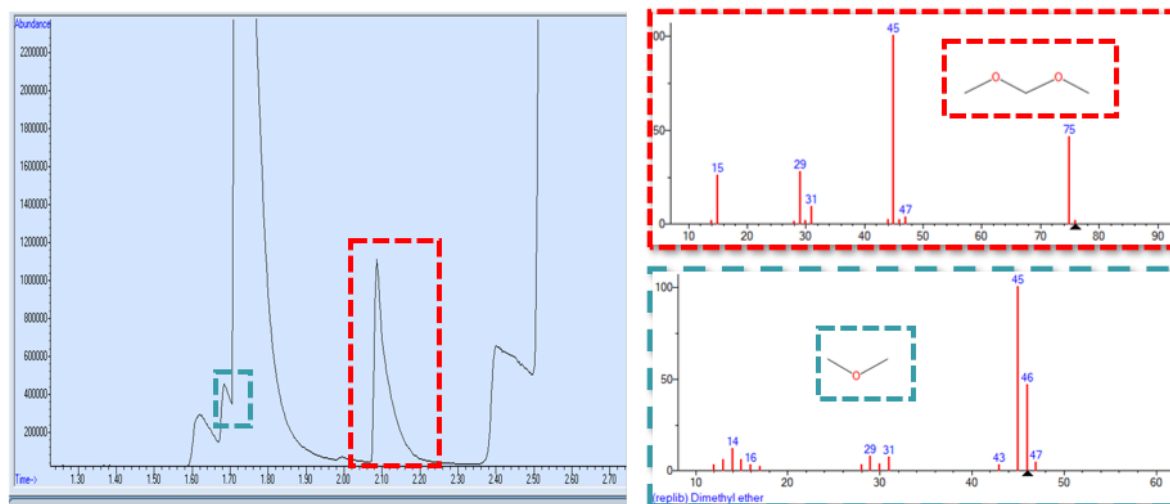


Fig. S8 GC-MS for H₃AuCl₄ salt in methanol. The results reveal the presence of Methylal (CH₃OCH₂OCH₃) and Dimethyl ether (CH₃OCH₃)

Table S1 Summary of some key observations in this study

Solvent	Environment (bulk or microdroplet)	Formation of Nanoparticles $M^{n+} + ne^- = M(s)$	Metal ions which form H_2O_2	Kinetics of Formation of Nanoparticles $M^{n+} + ne^- = M(s)$
Water	Bulk	Au and Pt nanoparticles	Au^{3+} , Pt^{4+} , Fe^{3+}	Fast
	Microdroplet			
Methanol	Bulk	Au and Pt nanoparticles	Au^{3+} , Pt^{4+} , Fe^{3+}	Fast
Ethanol	Bulk	Au and Pt nanoparticles	Au^{3+} , Pt^{4+} , Fe^{3+}	Fast
Acetonitrile	Bulk	Negligible NPs formation	No H_2O_2	Sluggish

Table S2:

Standard electrochemical series with the standard reduction potentials:

Standard Reduction Half-Reaction	Standard Reduction Potential E° (volts)
$\text{Au}^+ + e^- \rightleftharpoons \text{Au}(s)$	1.83
$\text{Au}^{3+} + 3e^- \rightleftharpoons \text{Au}(s)$	1.52
$\text{Au}^{3+} + 2e^- \rightleftharpoons \text{Au}^+$	1.36
$\text{AuCl}_4^- + 3e^- \rightleftharpoons \text{Au}(s) + 4\text{Cl}^-$	1.002
$\text{AuCl}_4^- + 2e^- \rightleftharpoons \text{AuCl}_2^- + 2\text{Cl}^-$	0.926
$\text{Pt}^{2+} + 2e^- \rightleftharpoons \text{Pt}(s)$	1.2
$\text{PtCl}_2 + 2e^- \rightleftharpoons \text{Pt}(s) + 4\text{Cl}^-$	0.78
$\text{PtCl}_4 + 2e^- \rightleftharpoons \text{PtCl}_2 + 2\text{Cl}^-$	0.75
$\text{Fe}^{3+} + e^- \rightleftharpoons \text{Fe}^{2+}$	0.771
$\text{H}_2\text{O}_2 + \text{H}^+ + e^- \rightleftharpoons \text{HO}^* + \text{H}_2\text{O}$	0.710
$\text{O}_2(g) + 2\text{H}^+ + 2e^- \rightleftharpoons \text{H}_2\text{O}_2$	0.695
$\text{O}_2(g) + 2\text{H}_2\text{O}(l) + 4e^- \rightleftharpoons 4\text{OH}^-$	0.401
$\text{Cu}^{2+} + 2e^- \rightleftharpoons \text{Cu}$	0.34
$\text{Fe}^{3+} + 3e^- \rightleftharpoons \text{Fe}(s)$	-0.037
$\text{Ti}^{2+} + 2e^- \rightleftharpoons \text{Ti}(s)$	-0.163
$\text{Ti}^{3+} + e^- \rightleftharpoons \text{Ti}^{2+}$	-0.37
$\text{Fe}^{2+} + 2e^- \rightleftharpoons \text{Fe}(s)$	-0.44
$\text{Zn}^{2+}(aq) + 2e^- \rightleftharpoons \text{Zn}(s)$	-0.76
$\text{Al}^{3+} + 3e^- \rightleftharpoons \text{Al}(s)$	-1.706
$\text{Mg}^{2+} + 2e^- \rightleftharpoons \text{Mg}(s)$	-2.356

Section S2: Confirmation of H₂O₂ peak position

To confirm that the obtained peak positioned at a chemical shift around 9.4 ppm in gold ion solution (0.3M H_{AuCl₄} in water) corresponds to the H₂O₂ only (Fig. S9), the peak was compared to one obtained for the same gold ion concentration (0.3M H_{AuCl₄}) with the addition of 200μM H₂O₂ (i.e., 0.3M H_{AuCl₄} + 200 μM H₂O₂) and the new peak was found at the same position/chemical shift with relatively more intensity and no other additional peak/s was found in the spectra. This confirms that the peak at around 9.4 ppm corresponds to H₂O₂ only.

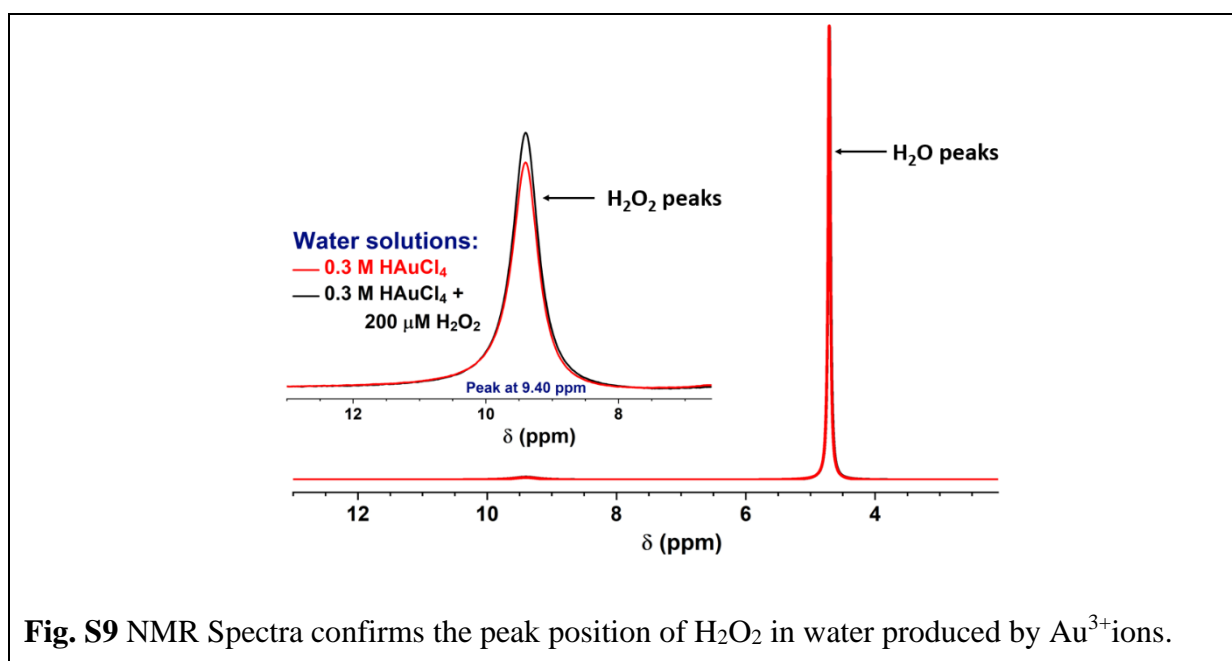
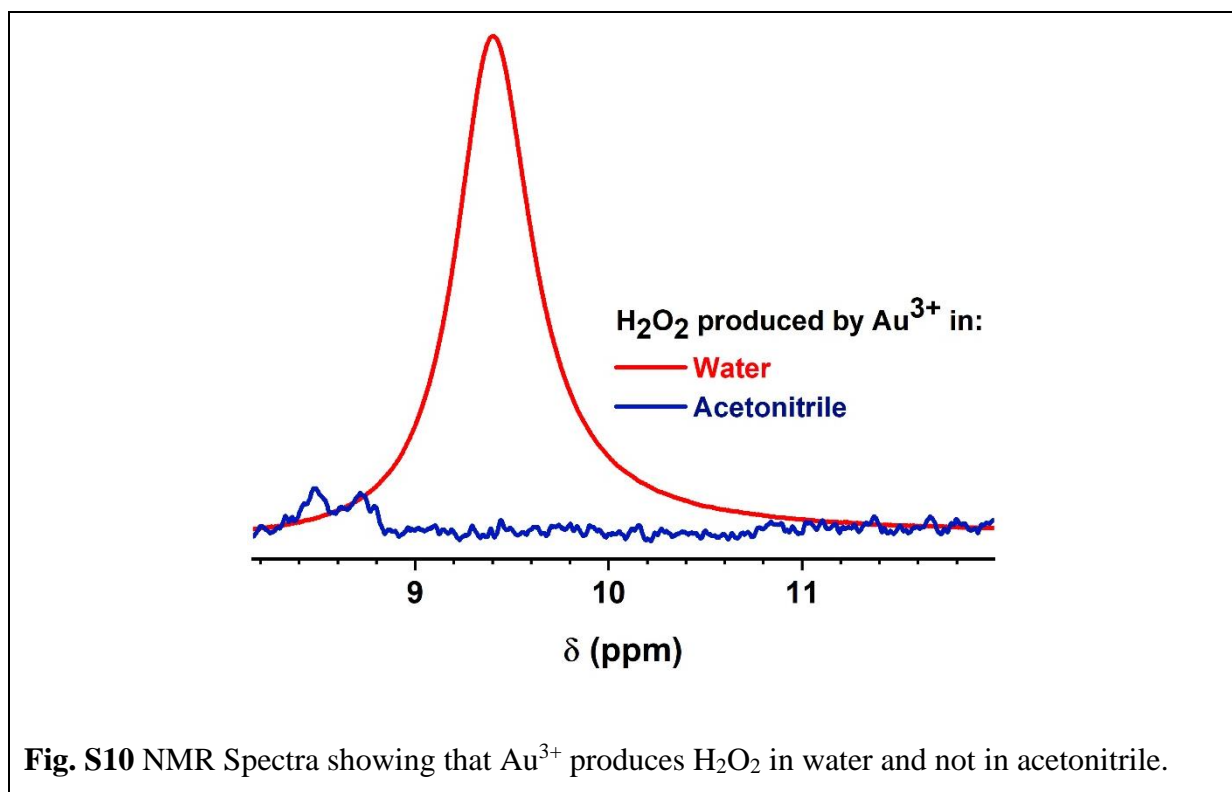


Fig. S10 shows the data obtained for the same concentration of gold ion (Au^{3+}) in water and acetonitrile, which confirmed the formation of H_2O_2 in water and not in acetonitrile.



References:

1. Gallo Jr A, *et al.* On the formation of hydrogen peroxide in water microdroplets. *Chemical Science* **13**, 2574-2583 (2022).
2. Eatoo MA, Mishra H. Busting the myth of spontaneous formation of H₂O₂ at the air–water interface: contributions of the liquid–solid interface and dissolved oxygen exposed: *Chemical Science* **15**, 3093-3103 (2024).